Eur. Phys. J. B **43**, 557–564 (2005)
DOI: 10.1140/epjb/e2005-00090-x

THE EUROPEAN PHYSICAL JOURNAL B

Anisotropic conductance of Pb–induced chain structures on Si(557) in the monolayer regime

C. Tegenkamp, Z. Kallassy, H.-L. Günter, V. Zielasek, and H. Pfnür[a]

Institut für Festkörperphysik, Universität Hannover, Appelstraße 2, 30167 Hannover, Germany

Received 1st December 2004
Published online 30 March 2005 –

Abstract. We present data of a study of four-point conductance of adsorbed Pb films on Si(557) in the thickness range between 0.6 up to several monolayers (ML) at various annealing stages. These measurements are combined with tunneling microscopy (STM). Onset of conductance is found close to the percolation limit. Pb layers annealed to room temperature are characterized by activated contributions to conductance up to 3 ML, a purely metallic temperature dependence at thicker layers, and an anisotropy of at most a factor of 2. On the contrary, annealing to 640 K, leaving only the first monolayer on the Si(557) surface results in extremely high surface state conductance which is quasi one–dimensional below a critical temperature of $T_c = 78$ K, associated with an order–disorder phase transition. Induced by a 10-fold superperiodicity along the Pb chains and their lateral ordering, the system switches from low to high conductance anisotropy, with a metal–insulator transition in the direction perpendicular to the chain structure, while in the direction along the chains conductance with a $1/T+$ const. temperature dependence was found.

PACS. 73.25.+i Surface conductivity and carrier phenomena – 68.37.Ef Scanning tunneling microscopy – 68.65.-k Low-dimensional, mesoscopic, and nanoscale systems: structure and nonelectronic properties

1 Introduction

One- or two-dimensional electronic systems are very interesting physical objects, since, due to the electron confinement, an increased electron correlation [1] leads to strong deviations from the Fermi liquid and formation of a Luttinger liquid [2,3]. Particularly in one–dimensional systems the enhanced interaction is accompanied by instabilities. Interactions between lattice, charge and spin cause formation of charge and spin density waves that lower the energy and lead to metal-insulator transitions in the electronic transport properties of such a system [1,4].

Already for the ideal systems it is clear that the electronic properties of low–dimensional systems are intimately related to their geometric structure. In real and very small one- or two-dimensional systems, this problem is modified by the fact that they must be supported by or embedded into a substrate material or stabilized by other means. Thus their realizations are always approximate using either strongly anisotropic crystals [5,6] and polymers [7], or supporting surfaces [8]. Adsorbed layers, which partly form chain structures on substrates like Si(111) [8,9], are alternative realizations that come closer to atomic chains, and allow precise access to the geometric and electronic properties of quasi-one-dimensional systems. Recent examples are submonolayers of Ag and Au atoms on vicinal Si(111) surfaces [10–12]. A property that makes these systems particularly interesting is in fact the coupling with the underlying substrate. The energetic, electronic and relaxational interplay between the inevitable embedding substrate material and the adsorbate determines even the effective dimensionality of such systems.

The Si(557) surface as substrate has already the striped structure with the alternation of (111) and (112) oriented micro-facets, which seems to be almost unchanged by the adsorption of lead (see also below). Thus electronic and geometrical properties can be well compared with those obtained on the flat Si(111) substrate, where magnetoconductive, and the correlation with geometric properties, have been studies extensively in the recent past [13,14]. Sign oscillations of the Hall constant as a function of the Pb layer thickness have been shown to be a quantum effect due to the discretization of the layer thickness and the corresponding changes of the two-dimensional bandstructure [15,16].

We will show in this paper that the (557) surface is able to superimpose its symmetry onto the adsorbed Pb layer, which under certain conditions – a detailed description is given below – forms chain structures so that transitions between one- an two-dimensional behavior can be studied with this system. On both facets the adsorption of Pb is known to modify only slightly the energetic position of

[a] e-mail: pfnuer@fkp.uni-hannover.de

occupied Si surface states at concentrations up to one monolayer (ML), which pin the Fermi level close to a mid-gap position [17]. Thus the underlying Si interface is always charge depleted irrespective of doping. Using an undoped Si sample we are thus able to measure almost pure surface state conductance even over macroscopic distances, as also corroborated by the measured Pb coverage dependence.

Here we present temperature dependent macroscopic DC conductivity measurements in the coverage range between submonolayers up to several layers of Pb obtained after different steps of annealing. Particularly remarkable are the results after a high temperature annealing step that desorbs all multilayers and leads to formation of a chain structure with just one monolayer of Pb. As revealed by tunneling microscopy (STM), switching between conductance with high and low anisotropy, respectively, is coupled with an order-disorder phase transition. A remarkably high conductivity along the chains in the highly anisotropic state is found which decreases as a function of temperature between 4 and 80 K. This behavior is exactly opposite to the typical occurrence of Peierls i.e. metal-insulator transitions to an insulating state at low temperature, as observed in comparable systems [9]. If such a transition occurs at all, it must be below 4 K.

2 Experiment

The experiments were carried out under ultra–high vacuum conditions at base pressures lower than 5×10^{-9} Pa in two separate vacuum chambers, set up for conductivity measurements at variable temperatures down to 3.5 K (apparatus A), and for tunneling microscopy at variable temperatures (apparatus B), respectively. In both chambers the average morphology was controlled by low energy electron diffraction (LEED), the cleanliness of the Si surfaces by STM and by Auger spectroscopy (AES). The Si(557) substrates (Crystec, Berlin) were chemically cleaned ex-situ. Atomically clean Si(557) surfaces were obtained after heating these substrates to 1370 K for 10 seconds in vacuum, followed by annealing for 15 minutes at 1030 K and slow cooling to 600 K. We note that long time annealing using temperatures higher 1370 K causes faceting of the surface, as seen by STM and LEED. Faceting can be avoided removing the native oxide by means of Si evaporation at 1170 K instead of using high temperatures [18]. This procedure was used in later experiments. Pb was evaporated from thermally heated Al_2O_3 crucibles, and the Pb coverage calibrated by conductivity measurements of thick Pb films grown on Si(111) substrates at 20 K [14] within an accuracy of 5% of a monolayer (ML).

In our experiments an extended four-point geometry was used (cf. with Fig. 1). The sample had eight predeposited macroscopic $TiSi_2$ contacts with a thickness of approximately 50 nm that are separated pairwise by slits machined into the samples as shown in Figure 1. The use of 8 contacts allowed exact symmetrization of the current parallel and normal to the step direction. By automatic switching between equivalent sets of contacts, the conductivity was measured sequentially parallel and perpendicular to the steps. The separation between equivalent contacts was approximately 10 mm. In all measurements contributions of the clean Si substrate (measured resistance 16 kΩ at room temperature, >500 kΩ below 150 K) were carefully subtracted.

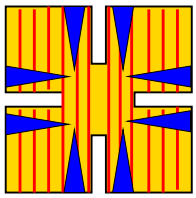

Fig. 1. Schematic drawing of the Si(557) samples with the arrangement of the eight $TiSi_2$ contact pads. The lines indicate the stripe structure along the $[1\bar{1}0]$ direction.

Detailed structural informations of the surface were obtained using a variable temperature STM (apparatus B, RHK 300 Series, temperature range between 40 K and 1400 K). The STM system consists of a preparation chamber, equipped with optical LEED and AES to control the morphology and the chemistry of the clean Si(557) surface and a separate chamber containing the STM. A load-lock system allows to change samples without breaking vacuum. The Pb evaporator was pointing directly towards the STM-stage to allow adsorption also at low temperatures. The calibration of film thickness was done using a quarz microbalance.

Using He evaporation cryostats, the samples were cooled down to 3.5 K in the conductivity apparatus, and to 40 K in the STM machine. The temperature was measured with calibrated silicon diodes, in apparatus A on the cryostat and with a thermally completely shielded sample, and in machine B directly on a dummy sample. The annealing temperature was determined by attaching a Chromel-alumel thermocouple to the center of a dummy sample for calibration of the IR pyrometer used for the actual measurements. The temperature was thus determined within an accuracy of ±2 K. Reproducibility was in the same range of uncertainty.

3 Results and discussion

3.1 Conductance after low temperature annealing

For Pb layers evaporated onto the Si(557) samples at low temperature (below 25 K) onset of measurable Pb induced conductance was found close to 0.6 ML (ML given with respect to the density of Si surface atoms). Annealing to temperatures close to room temperature leads to an increase of conductance (except at coverages close to the percolation threshold, where no effect was detected) and to reversibility of conductance as a function of temperature below room temperature. Only the conductance curves after this annealing step are shown in Figure 2 for different initial Pb coverages.

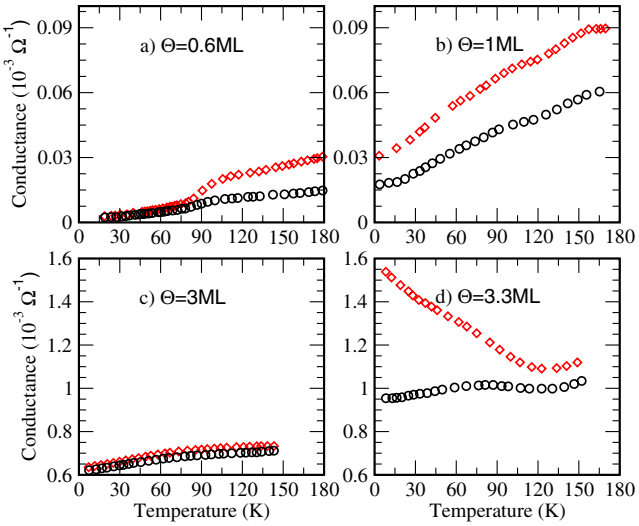

Fig. 2. Conductance as a function temperature for different Pb coverages after annealing the layers to room temperature. a) 0.6 ML, b) 1 ML, c) 3 ML and d) 3.3 ML. Diamonds are for the $[1\bar{1}0]$ direction ($\sigma_{\parallel}$), circles for the $[\bar{1}\bar{1}2]$ direction ($\sigma_{\perp}$) normal to the step edges.

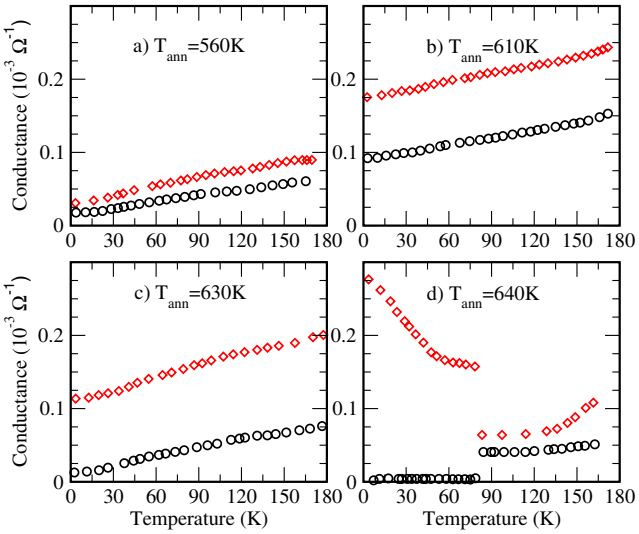

Fig. 3. Changes of conductance properties after different annealing steps for an initial coverage of 1 ML Pb: a) annealing to 560 K, b) to 600 K, c) to 630 and d) to 640 K. Symbols are the same as in Figure 2.

Up to three monolayers, the conductance increases as a function of temperature. This increase in all measured curves, however, is much weaker than exponential, indicating the existence of many different activation barriers with a distribution of activation energies. Already at coverages above one monolayer there is a significant metallic, i.e. non-activated, contribution, estimated from the extrapolation $T \rightarrow 0$. At three ML this contribution dominates strongly over the activated part, which disappears completely at Pb coverages above 3.5 ML (see Fig. 2d for the 3.3 ML case).

The low symmetry of the Si(557) surface is also reflected in the anisotropy of conductance. Conductance is always smaller in the $[\bar{1}\bar{1}2]$ direction normal to the step edges. At a Pb coverage of $\Theta = 0.6$ ML the ratio $\sigma_{\parallel}/\sigma_{\perp}$ is about 2 above 100 K, whereas it is typically around 1.5 at higher coverages. The activated contribution in $\sigma_{\parallel}$ obviously vanishes at lower coverages as that in $\sigma_{\perp}$, as seen from Figure 2d, which is another consequence of the anisotropy of the surface.

This behavior, apart from the anisotropy, is qualitatively similar to that found for Pb layers on flat Si(111) surfaces [14]. Here again purely metallic behavior was found at coverages above 4 ML. On the flat surface, all films up to 4 ML are characterized by a high degree of disorder [13], rationalizing the distribution of activation barriers.

3.2 Conductance after high temperature annealing

The behavior shown in Figure 2 is not changed qualitatively when the layers are annealed to higher temperatures below 600 K. The effect of annealing to various temperatures is demonstrated as an example for a Pb coverage of 1 ML in Figure 3. Annealing to temperatures above 600 K first clearly increases conductivity, and the relative contribution of the activated part to conductance is reduced, but still dominates the temperature behavior. An obvious explanation is that annealing reduces the density of defects in the Pb layer. Qualitatively the same behavior is found for annealing at temperatures up to 630 K for several minutes. In all cases the weak anisotropy of conductance parallel and perpendicular to the step direction is maintained.

This behavior of a weak anisotropy and a gradual increase of conductance as a function of temperature is changed drastically by the annealing step to 640 K. The curves obtained after this high temperature annealing step are now dominated by an abrupt change at a temperature of 78 K, separating a high temperature region with small conductance anisotropy (factor ≈ 1.5) from the low T region which is characterized by high anisotropy (factor 30 to 60). At temperatures below 78 K a stepwise increase of $\sigma_{\parallel}$ by typically a factor of 3 is observed, whereas $\sigma_{\perp}$ drops sharply by a factor of 2 to 10, as seen in Figure 3d. This final step of annealing obviously induces two effects: The monolayer undergoes an ordering process that is strongly activated so that it occurs only during annealing to temperatures close to desorption. The alternative that mixing of Si and Pb atoms in the first layers takes place, so that a surface silicide is formed, is unlikely from the STM data presented below. This will be discussed there. Only this ordered layer is able to undergo the phase transition close to 80 K, which switches the system from low conductance anisotropy to high anisotropy.

This switching behavior of conductance shown in Figure 3d was found to be independent of the initial Pb coverage, Θ_{ini}, after the high temperature annealing step to 640 K, if Θ_{ini} exceeded 1 ML. We performed tests with initial coverages between 0.6 and 20 ML (see also

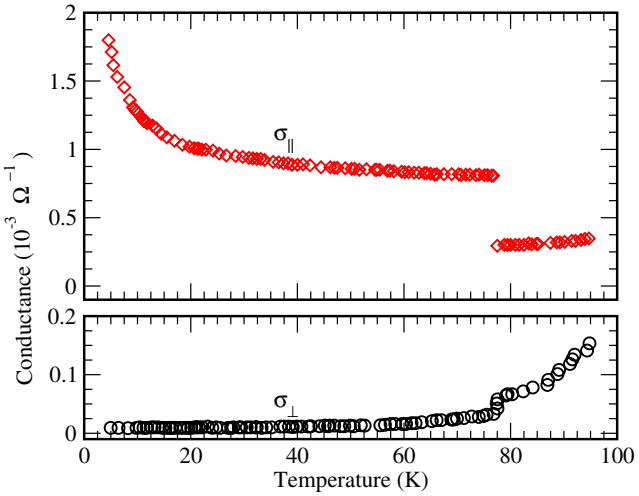

Fig. 4. Temperature dependence of the dc-conductance after adsorption of 4 ML and annealing to 640 K, measured along the $[\bar{1}\bar{1}2]$ ($\sigma_\perp$) and the $[1\bar{1}0]$ direction ($\sigma_\parallel$).

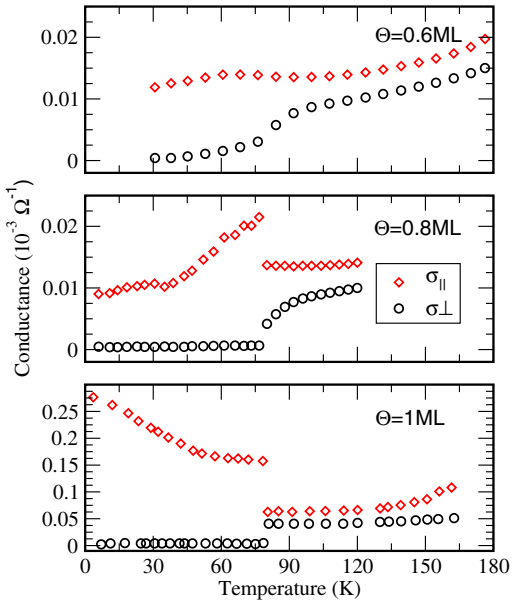

Fig. 5. Temperature dependence of conductance after adsorption and annealing to 640 K of 0.6 of Pb (top), 0.8 ML (middle) and 1.0 ML annealing to 640 K. Squares indicate $\sigma_\parallel$, circles $\sigma_\perp$.

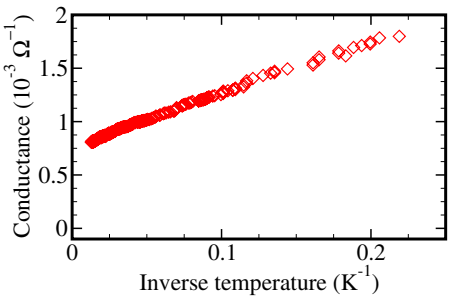

Fig. 6. $\sigma_\parallel$ below 78 K from Figure 4, plotted versus 1/T.

below). Also the conductance values quantitatively obtained were found to be independent of the initial coverage for layers thicker than 3 ML. An example with Θ_{ini} = 4 ML and annealing to 640 K is shown in Figure 4. Comparing with Figure 3d, the main difference is in the absolute values of conductance, which are a factor of 6 higher for $\sigma_\parallel$ in Figure 4 over the entire temperature range. However, the critical temperature of the phase transition, switching between low and high anisotropy, is exactly the same in both graphs, as is the relative magnitude of conductance change in $\sigma_\parallel$ at the phase transition. The changes in $\sigma_\perp$ are more gradual in Figure 4. These data were measured on a different sample than that in Figure 3 so that variations of the defect density between different samples can be the reason for this difference.

The vapor pressure of bulk Pb at 640 K is 7×10^{-7} mbar [19]. This means that after annealing for several minutes all multilayers of Pb must have been desorbed. A direct Auger calibration carried out by us corroborates this assumption. It yields a residual Pb coverage of 0.9 ± 0.1 ML after the 640 K annealing step. This directly explains the insensitivity of the conductance results to the initial coverage in the multilayer range after the high temperature annealing step. The property that conductance can be switched, driven by temperature, from high to low anisotropy is therefore a property of the monolayer of Pb and/or of the conductance channels induced by the Pb monolayer on the Si(557) surface. It seems that higher initial coverages (above one monolayer of Pb) only yield a higher probability for connecting conducting channels along the $[1\bar{1}0]$ direction to the contacts. The assumption of monolayer coverage is fully compatible with the STM results described below. As seen there, atomic wire-like structures are formed after this high temperature annealing step that are responsible for the anisotropy of conductance observed at low temperature.

More details can be learned by a study of the coverage dependence of conductance after the high temperature annealing step. Results of the temperature dependence of conductance after annealing each layer to 640 K are shown for initial coverages of 0.6 ML, 0.8 ML and 1.0 ML (from top to bottom) in Figure 5. Little changes are observed in the conductance of the 0.6 ML layer. Its absolute value above 100 K remains the same as without annealing. It is strongly activated also after annealing with a small increase of anisotropy in the temperature range below 100 K. The sharp phase transition observed at initial coverages of 1 ML and higher, however, occurs already with an initial coverage of 0.8 ML. Already at this coverage the abrupt change of conductance occurs with a similar relative magnitude as at higher initial coverages. The temperature dependence of $\sigma_\parallel$ below T_c, however, is reversed: It increases as a function of temperature, starting from a very low value around 10^{-5} Ω^{-1}.

For the "optimal" conductance curves after annealing, i.e. those obtained with initial Pb coverages of 3 ML or more, $\sigma_\parallel$ below T_c can be well described by $\sigma_\parallel = A + B \times T^{-n}$ with n close to 1 (see Fig. 6). This decrease of $\sigma_\parallel$ as a function of temperature contrasts with

the increase above the jump at 78 K, indicating thermally activated behavior above this threshold. $\sigma_\perp$, on the other hand, is thermally activated in both temperature regimes. Whereas for $\sigma_\perp$ defects may play some role as mentioned, the optimal conductance values of $\sigma_\parallel$ did not vary between different samples, and neither the abrupt changes seen in the conductance at 78 K nor the temperature dependence of $\sigma_\parallel$ below 78 K can be explained by defects. Since we cannot expect that a surface is free of defects like point defects or steps, at least on the atomic scale, such defects cannot act as effective scatterers along the Pb chains.

This property changes when the coverage is so small that only very few chains are lefts that form a conducting channel between the contacts of our experimental setup. Here there is a high probability for more extended defects that can only be surmounted by thermal activation. This scenario seems to be valid at a Pb concentration of 0.8 ML and lower. The observed jump in conductance at T_c and the increase of $\sigma_\parallel$ as a function of temperature below T_c is compatible with the assumption of sections of isolated chains separated by gaps that can still be surpassed by thermal activation.

3.3 Correlation of conductance with geometrical properties

As mentioned, we performed STM investigations of identically prepared samples in a different chamber. Figure 7 shows an STM image of the clean Si(557) surface consisting of an alternating arrangement of short (111)– and (112)–facets with an average hill-valley spacing of 57 Å according to the model of reference [20]. This model is supported by LEED, which shows the characteristic 7×7 reconstruction of (111) facets [21,22] and the known 2×1 reconstruction of Si(112) surfaces [23]. Microscopically, the (111) facets are separated by 3-fold steps. As seen from this figure, the typical terrace lengths that can be obtained on these samples are around 200 nm. Neighboring terraces are separated by steps that correspond to steps of 6 and 9 atomic heights. They also contain kinks, as also seen in this figure. In any case, these extended line defects remain on the atomic level. Even with the low density of terraces shown in Figure 7 many thousand steps intersect the path between two contacts in our experimental setup.

As judged from a large series of adsorption experiments and various annealing steps, adsorbed Pb leaves the terrace structure of the Si(557) sample unaltered. After adsorption of Pb at low temperatures and annealing for 15 minutes at 640 K, STM reveals the characteristic chain structure shown in Figure 8 with an average spacing between the chains of 14 Å. This chain structure is found only after this high temperature annealing step, whereas a more irregular bumpy hill-and-valley structure is found at lower annealing temperatures. The chain structure is destroyed by annealing at 650 to 660 K. Thus there is a close correlation between the chain structure observed here, and the strongly anisotropic conductance behavior found below 78 K at one monolayer coverage. The surface shown in Figure 8 is completely covered with Pb, and all

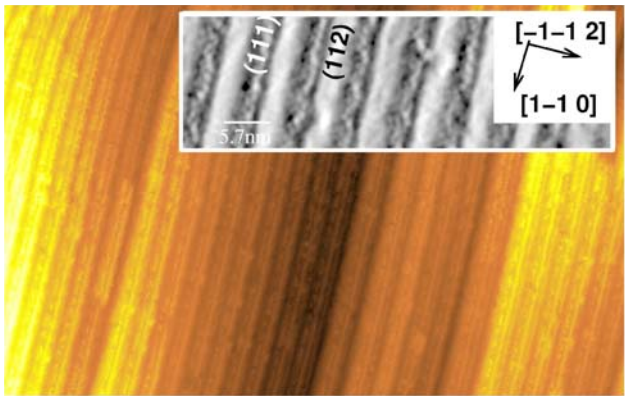

Fig. 7. STM picture (180 nm × 115 nm) of the clean Si(557) surface. From the inset (derivative, 50 nm × 15 nm) the alternating arrangement of (111)- and (112)-facets can be seen. Sample bias voltage +2 V, 0.5 nA.

chain structures are Pb induced. This is obvious from the disappearance of the double–line structure on the clean Si(557) surface, which is attributed to the (112) facets, but also from small minority areas, where, presumably induced by defects, Pb is desorbed completely, and the bare (111) facets are visible with their characteristic 7×7 reconstruction. Therefore, these chains are unambiguously induced by Pb and they are responsible for the metal–insulator and insulator–insulator transitions of the conductance along the $[\bar{1}\bar{1}2]$ and $[1\bar{1}0]$ directions, respectively.

As judged from the slightly different contrast, also at other tunneling voltages, and from their stability as a function of temperature, it seems that two different kinds of chains on the surface can be discriminated, which may be attributed to chain formation on the two facets. As judged from chains ending at small clean 7×7 islands, the bright chains must be located on the (111) facets or at the edge between the two facets, whereas the other chains must be on the (112) facets. The step–step distance there is around 10 Å on the clean surface, i.e. significantly smaller than the Pb-Pb chain separation. This enlarged chain distance can be caused by effective lateral repulsion between the wires so that they are not located at equivalent positions on each mini-terraces, supporting the assumption of coupled chains. As an alternative, the step separations on the original (112) facets, induced by Pb and high temperature annealing, could be enlarged at the expense of the extension of the (111) facet. If this rearrangement of the local step structure is necessary, it would explain the necessity for high temperature annealing. Of course, also the simultaneous contribution of both mechanisms is possible, but STM does not allow to discriminate between them unambiguously. In any case, it is obvious that each Pb wire consists of more than one atomic chain in order to accommodate the Pb concentration of approximately 1 ML.

Even at a temperature of 40 K these chains contain a lot of defects that limit the typical undistorted length of a chain to 30 up to 100 nm, with the bright chains containing typically less defects than the others. Whereas the chain separation has a well defined value,

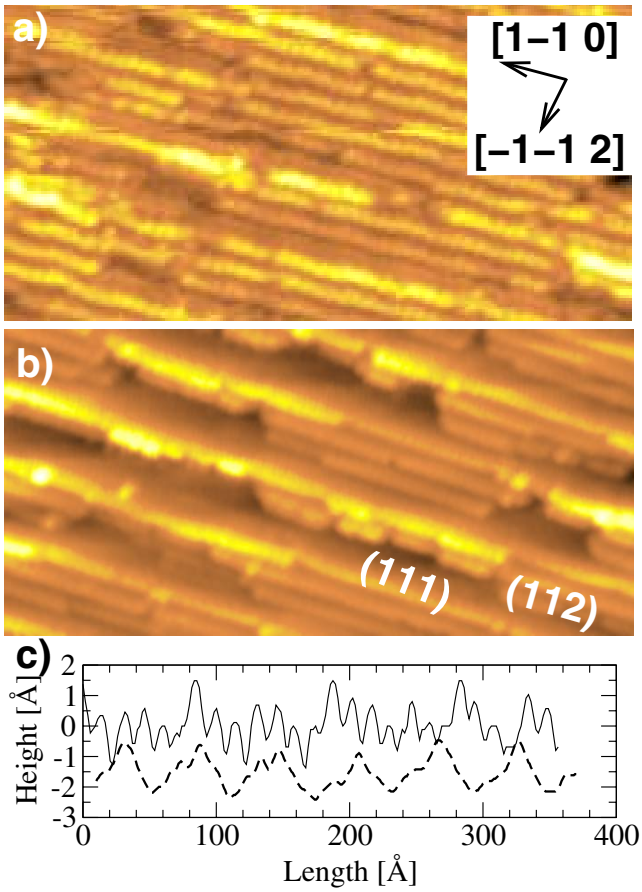

Fig. 8. STM picture (40 nm × 20 nm) of the chains after adsorption of 10ML Pb/Si(557) and annealing to 670 K. Temperature of measurement: a) 40 K, b) 100 K. The solid curve in c) shows a line scan along the $[\bar{1}\bar{1}2]$ direction taken from a). The dashed curve represents a line scan of the clean Si(557) surface.

the stacking sequence normal to the chains seems to follow the local variation of facet sizes so that it is not long range ordered. Together with the step and kink structure of the substrate (not shown) these findings exclude the possibility of a macroscopic extension of undistorted chains from one contact to the other of the conduction measurements.

Nevertheless, the formation of the Pb induced chain structures is intimately related to the observed behavior of conductance, and, in particular, to the drastic changes in anisotropy. The abrupt changes observed at $T_c = 78$ K cannot be explained by chain formation alone, but must be due to changes in local structure and/or to a possible structural phase transition. Indeed, clear changes in the local correlations become visible by taking STM images above and below T_c, i.e. by filling the cryostat either with ℓHe or with ℓN_2 so that lowest temperatures on the sample of 40 K and 100 K were obtained, respectively (see Figs. 8a, b). To examine correlation effects along and between the wires, one–dimensional Fourier transformations along and perpendicular to the chain structures were carried out on representative STM areas. The results are shown in the top part of Figure 9 for a typical single scan.

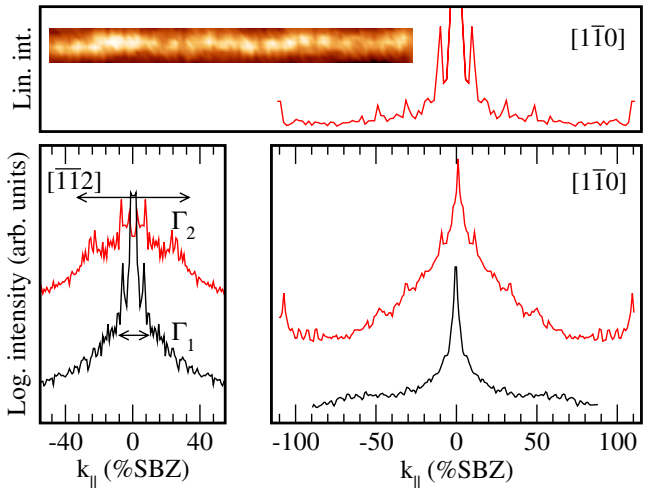

Fig. 9. Lower panels: Fourier transformations of line scans from STM pictures at 100 K (lower curves) and at 40 K for the direction perpendicular and parallel to the steps, respectively. In the top panel a single atomic chain and its Fourier transformation on linear scale is shown.

Averages over an area of 40 × 40 nm^2 are shown on log scale in the lower two panels.

Starting with the direction normal to the chains (left part of Fig. 9), for both temperatures a clearly enhanced Fourier component Γ_1 is seen that corresponds to the average hill and valley spacing of 57 Å, i.e. to the periodicity of the clean Si(557) surface. For $T = 40$ K an additional, but considerably broader component Γ_2 is seen, which corresponds to the 14 Å spacing of the Pb wires.

Parallel to the chain structure the Fourier transforms calculated from 40 K STM images show, in contrast to those of STM images taken 100 K, an additional periodicity with a fundamental wavelength of 10 times the next neighbor separation of Si, together with higher harmonics. The peak at 110% SBZ corresponds to the nearest-neighbor spacing of Pb with approximately the bulk Pb lattice constant. Little correlation of this periodicity between different chains was found. The modulation of the chains is weak, as obvious from Figures 8 and 9. It cannot be induced by missing Pb atoms, as seen, e.g., for the case of Ga on Si(112) [24], but rather by a modulation of the local position of adatoms, most likely due to the misfit between Si and Pb lattice constants. Since the lattice constant of Si is 9% larger than the lattice constant of Pb, registry between the ideal Si and Pb lattice is obtained every ten Si atoms, which agrees well with the ten–fold periodicity found.

Approaching T_c from high temperature, it seems to be the locking of the chains into the high order commensurate superperiodicity, coupled with a regular separation between the Pb induced chains, that cause the switching from low to high anisotropy and into a highly conducting state along the chains with a “metallic”-like temperature dependence.

As a first approach, i.e. neglecting all imperfections and defects, this anisotropic Pb monolayer can be

considered as a system of coupled Pb chains. Electrical conduction occurs in the partially filled band of Si surface states that is modified by the adsorbed Pb chains that impose their symmetry and their periodicity onto this band. As judged from the low electrical conductivity in the $[1\bar{1}0]$ direction in the low temperature regime and its temperature dependence, coupling is rather weak between the chains, and the electrons close to E_F are preferably localized within one chain. Along the chains, the 10-fold periodicity imposes a mesoscopic modulation that effectively backfolds the bandstructure of the unmodulated chains. Thus the effective Fermi wavelength, λ_F, cannot be smaller than twice the modulation period, but may be even much longer. Although only quantitative calculations, using, e.g., density functional theory, will be able to determine λ_F, backfolding in the bandstructure and the corresponding effective increase of λ_F can rationalize why these electrons are quite unsusceptible to local defects on the atomic scale along the chains. Although defects are present, they do not lead to localization of the conducting electrons along the wires down to temperatures of 4 K.

Passing the phase transition, also the conductance normal to the Pb chains drops sharply, but here the activated temperature behavior seen above the phase transition remains also at temperatures below. This strong anisotropy means a strongly enhanced localization of the electrons in the direction normal to the wires. One may even speculate that the conductance in this direction will be zero without presence of any defects. Although our present experiments cannot give a unique answer to this question, it is clear that the locking into a structure with a well defined separation of the Pb chains below T_c is of equal importance for the anisotropy of conductance as is the superperiodicity along the chains. Thus, the loss of correlation both along the chains, leading to the disappearance of the modulation, and perpendicular to them, which leads to an increase of perpendicular conductance by crossing the phase transition, brings conductance back to an only slightly anisotropic behavior.

In this context, it is interesting to note that above the phase transition both $\sigma_\parallel$ and $\sigma_\perp$ return to activated behavior, i.e. to an increased sensitivity to local defects. This fits qualitatively to the model of a much shorter effective λ_F in both directions in the high temperature phase than at low temperatures.

The conductance behavior in the highly anisotropic state may be a candidate for Luttinger liquid behavior in coupled chains [25]. Since we observe the quasi one-dimensional conductivity down to 4 K, the energy scales for two-dimensional coupling are extremely small (of the order of a few Kelvin or even less) compared with standard quasi one-dimensional conductors [26]. This suggests that we have found a system with almost ideal one-dimensional conductive properties.

On the other hand, the quantitative properties deviate clearly from the predictions for dc conductance in a Luttinger liquid, even in presence of defects [27], since a simple power law cannot be fitted to the data of $\sigma_\parallel$ below T_c. It can only be fitted to the data, if we subtract a comparatively large constant (see Fig. 6) from the data. If we neglect this constant, the 1/T behavior of $\sigma_\parallel$ is indicative of a Luttinger liquid with strong electron interactions of fairly long range. The meaning of the (still one-dimensional) "background" conductance must remain open at this point.

Significant coupling between the chains must also exist, as indicated by the nonzero value of $\sigma_\perp$ and its increase as a function of temperature. The temperature dependence found in our experiments for $\sigma_\perp$, can again not be described by a power law in T, as suggested for coupled Luttinger liquids [26,28]. Whether defects like additional steps – impurities can be excluded – are important for this deviation, cannot be answered at the moment, but this question may be accessible by miniaturizing the experimental setup, which is planned.

4 Conclusions

Concluding, quasi-metallic quasi-one-dimensional conductance with extremely high values of conductance can be obtained with only one monolayer of Pb that forms a chain structure on Si(557). Conductance can be switched from low to high anisotropy by an order-disorder phase transition with a mesoscopic modulation period. Thus, and in strong contrast to the metal-insulator transitions seen in most systems when temperature is decreased, we observe transitions from a quasi one-dimensional metal at low temperature to an insulator (with temperature activated behavior) at high temperature parallel to the Pb chains, and an insulator–metal transition in the direction normal to the Pb chains.

Although the low temperature system is highly anisotropic, the temperature dependence found deviates from the standard predictions for Luttinger liquids. The role of defects, although with seemingly small influence on the conductivity parallel to the chains, must be clarified in further experimental studies on a much smaller scale so that individual defects and their influence on conductance can directly be detected. Such experiments seem to be feasible with modern nanoscale techniques.

References

1. J. Voit, Rep. Prog. Phys. **58**, 977 (1995)
2. J.M. Luttinger, Phys. Rev. **119**, 1153 (1960)
3. F.D. Haldane, J. Phys. C: Solid State Phys. **14**, 2585 (1981)
4. R.E. Peierls, *Quantum theory of solids* (Clarendon, Oxford, 1955)
5. D. Jérome, Chemica Scripta **17**, 13 (1981)
6. R. Claessen et al., Phys. Rev. Lett. **88**, 096402 (2002)
7. S. Roth, W. Graupner, Synthetic Metals **57**, 3623 (1993)
8. F.J. Himpsel et al., J. Phys. C **13**, 11097 (2001)
9. T. Tanikawa, I. Matsuda, T. Kanagawa, S. Hasegawa, Phys. Rev. Lett. **93**, 016801 (2004)
10. J.R. Ahn, H.W. Yeom, H.S. Yoon, I.-W. Lyo, Phys. Rev. Lett. **91**, 196403 (2003)

11. J.N. Crain et al., Phys. Rev. Lett. **90**, 176805 (2003)
12. J.N. Crain et al., Phys. Rev. B **69**, 125401 (2004)
13. A. Petkova, J. Wollschläger, H.-L. Günter, M. Henzler, Surf. Sci. **482-485**, 922 (2000)
14. O. Pfennigstorf, A. Petkova, H.-L. Günter, M. Henzler, Phys. Rev. B **65**, 045412 (2002)
15. I. Vilfan, M. Henzler, O. Pfennigstorf, H. Pfnür, Phys. Rev. B **66**, 241306 (2002)
16. I. Vilfan, H. Pfnür, Eur. Phys. J. B **36**, 281 (2003)
17. D.A. Ricci, T. Miller, T.-C. Ciang, Phys. Rev. Lett. **93**, 136801 (2004)
18. M. Czubanowski, C. Tegenkamp, H. Pfnür, Appl. Phys. Lett. **84**, 350 (2004)
19. *Methods in Experimental Physics*, Vol. 14 of *Vacuum Physics and Technology* (Academic Press, New York, 1979)
20. A. Kirakosian et al., Appl. Phys. Lett. **79**, 1608 (2001)
21. E. Hoque, A. Petkova, M. Henzler, Surf. Sci. **515**, 312 (2002)
22. M. Henzler, R. Zhachuk, Thin Solid Films **428**, 129 (2003)
23. X.-S. Wang, W.H. Weinberg, Surf. Sci. **314**, 71 (1994)
24. A.A. Baski, S.C. Erwin, L.J. Whitman, Surf. Sci. **423**, L265 (1999)
25. S. Biermann, A. Georges, T. Giamarchi, A. Lichtenstein, *Strongly Correlated Fermions and Bosons in Low Dimensional Disordered Systems* (Kluwer, Dordrecht, 2002), p. 81
26. M. Dressel, K. Petukhov, B. Salameh, P. Zornoza, T. Giamarchi (2004), preprint `cond-mat/0409322`
27. T. Giamarchi, H. Schulz, Phys. Rev. B **37**, 325 (1988)
28. A. Georges, T. Giamarchi, N. Sandler, Phys. Rev. B **61**, 16393 (2000)